Supporting Information

Organic Piezocatalyst Polyimide: Molecular Structure Tailoring and Robust Built-in Electric Field

Yan Zhang,[a] Jingang Liu,[*a] Cheng Hu,[a] Xinxin Zhi,[a] Zhen Pan,[a] Hongjian Yu,[*b], Jie Han [b] and Hongwei Huang [*a]

[a] Engineering Research Center of Ministry of Education for Geological Carbon Storage and Low Carbon Utilization of Resources, Beijing Key Laboratory of Materials Utilization of Nonmetallic Minerals and Solid Wastes, National Laboratory of Mineral Materials, School of Material Sciences and Technology, China University of Geosciences, Beijing 100083, China
[b] School of Chemistry and Chemical Engineering, Yangzhou University, Yangzhou 225002, China

E-mail: liujg@cugb.edu.cn; yhj@yzu.edu.cn; hhw@cugb.edu.cn

1. Experimental details

1.1. Chemicals

Pyromellitic dianhydride (PMDA, 99%) was purchased from Shijiazhuang HOPE Chem. Co. Ltd. (Shijiazhuang, China) and dried at 180 °C in vacuum for 24 h prior to use. Melamine (99%) and hexadecyl trimethyl ammonium bromide (CTAB. 99%) was purchased from Aladdin (Shanghai, China) and used as received. Rhodamine B (RhB, 98%+) and tetracycline hydrochloride (TC, 98%) was purchased from Macklin reagent (Shanghai, China). Extra dry *N, N*-dimethylformamide (DMF, 99.9%), ethylene glycol (EG, 99%) and other chemicals (analytical pure) was purchased from Beijing Yili Fine Chemicals (Beijing, China). All of the reagents were used without further purification. Melem was obtained by treatment with melamine at 425° for 4h according to the procedure reported in the literature.[1]

1.2. Calculations and simulation

The theoretical calculations in this work were performed on the basis of extensive Density Functional Theory (DFT) calculations. The molecular structures were geometrically optimized using the functional hybrid B3LYP and the 6-31G (d, p) basis set in the Gaussian 09 program package. The dipole moments and molecular orbitals were calculated using the functional hybrid B3LYP and the 6-311G (d, p) basis set. Finite element method (FEM) calculations were performed using COMSOL Multiphysics 5.4 with the module of piezoelectric device based on the steady-state study.

2. Supplementary Figures

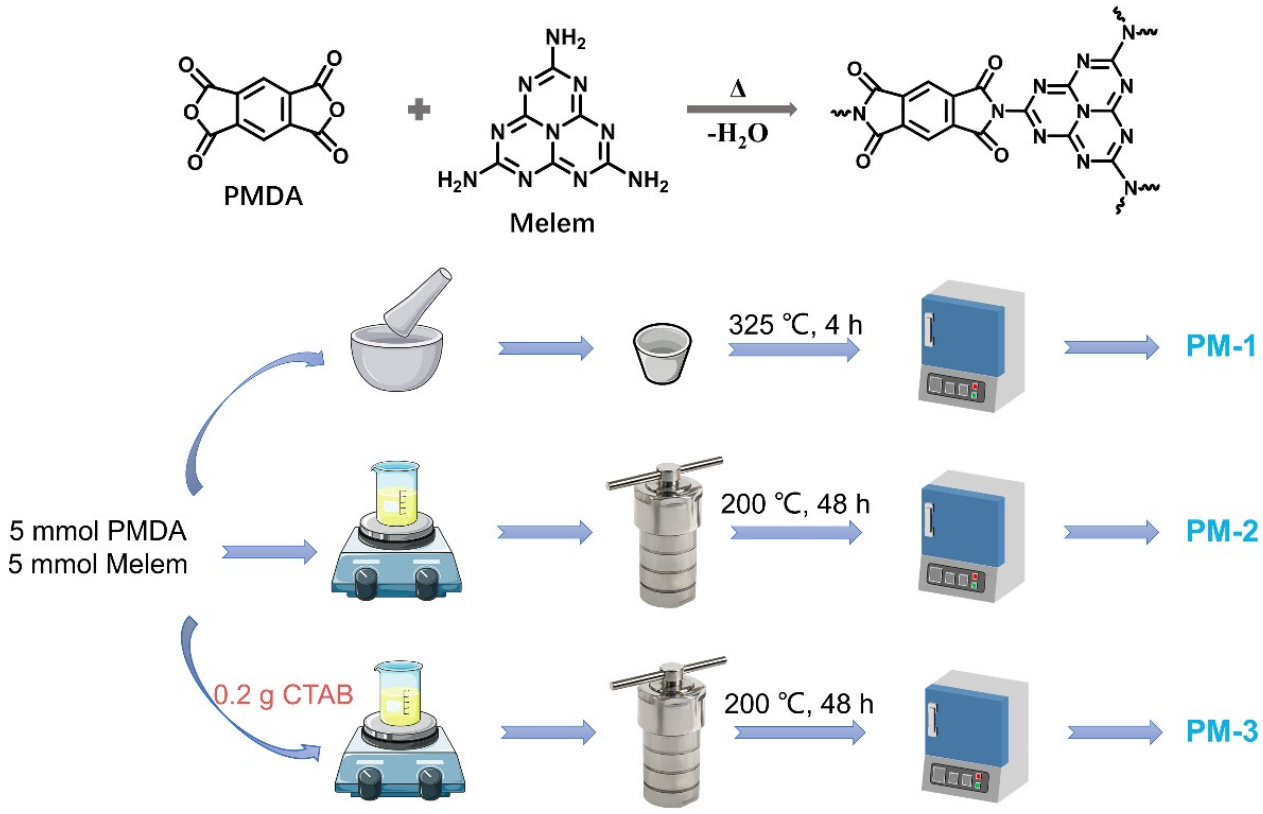

Figure S1. The synthesis routes of the three PI piezocatalysts.

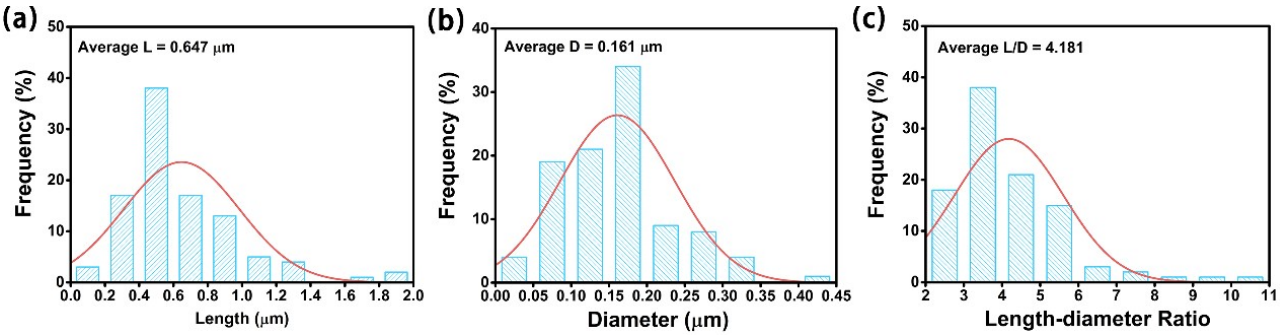

Figure S2. (a) Length distribution, (b) diameter distribution and (c) L/D ratio of PM-2.

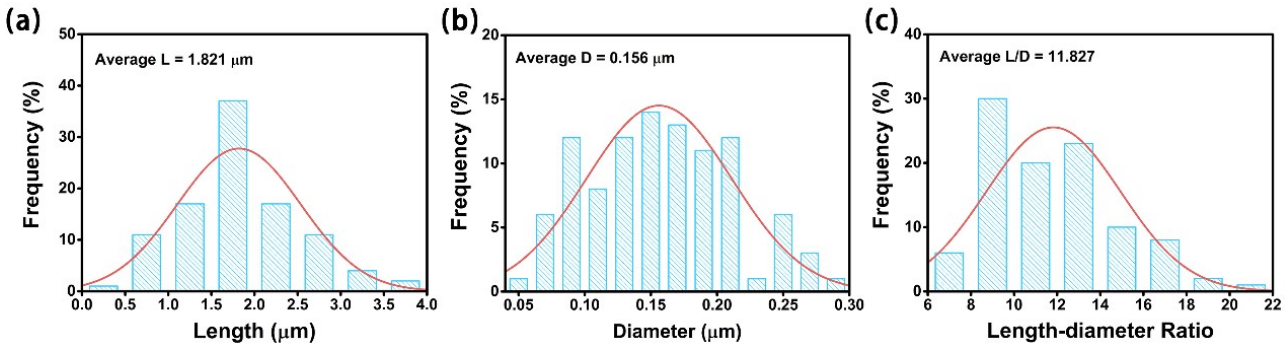

Figure S3. (a) Length distribution, (b) diameter distribution and (c) L/D ratio of PM-3.

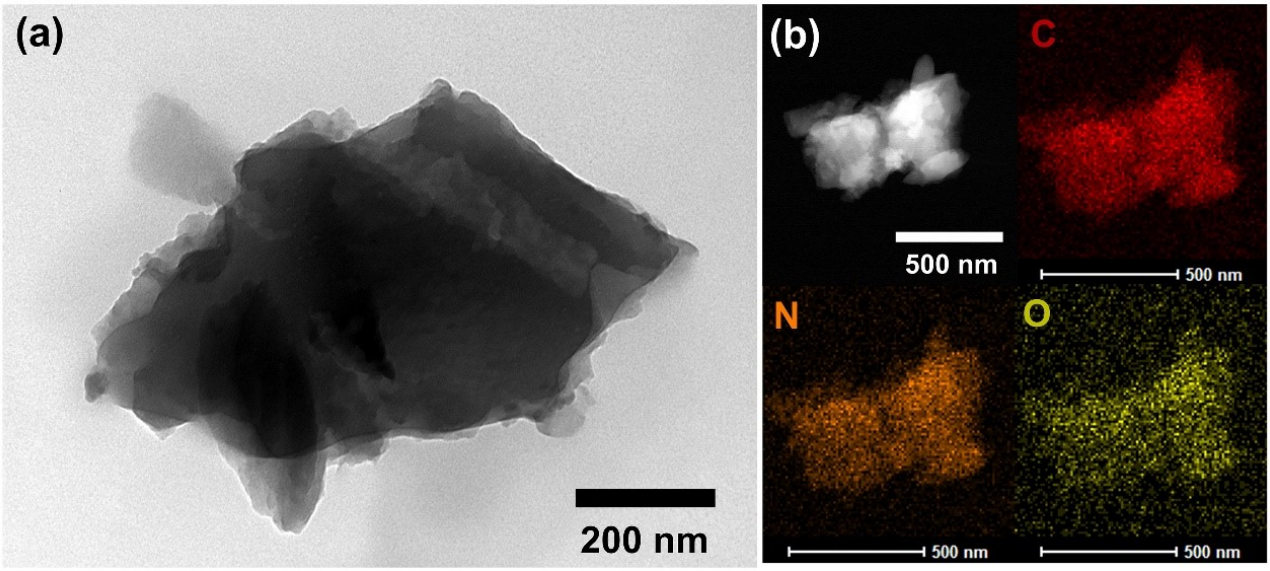

Figure S4. (a) TEM image (b) EDS elemental mappings of PM-1.

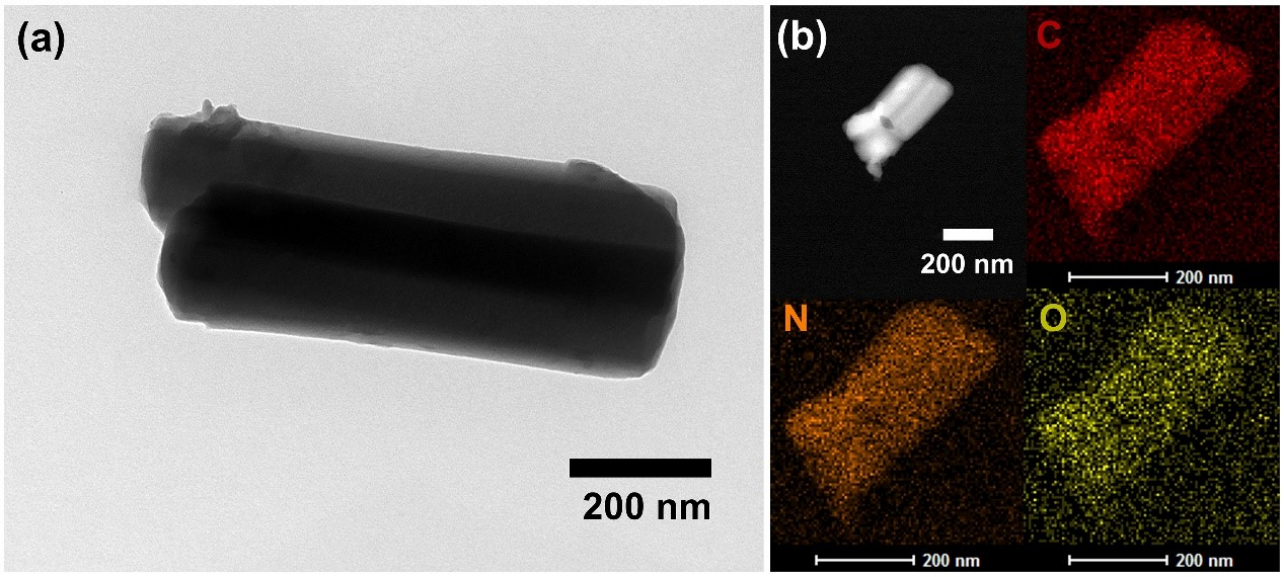

Figure S5. (a) TEM image (b) EDS elemental mappings of PM-2.

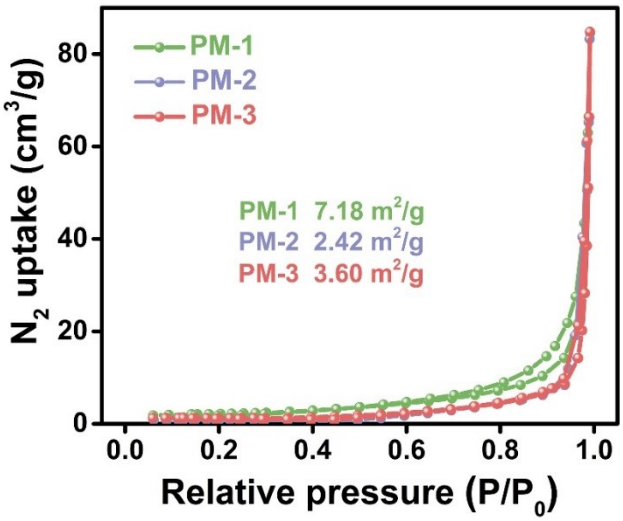

Figure S6. The N_2 adsorption-desorption isotherms.

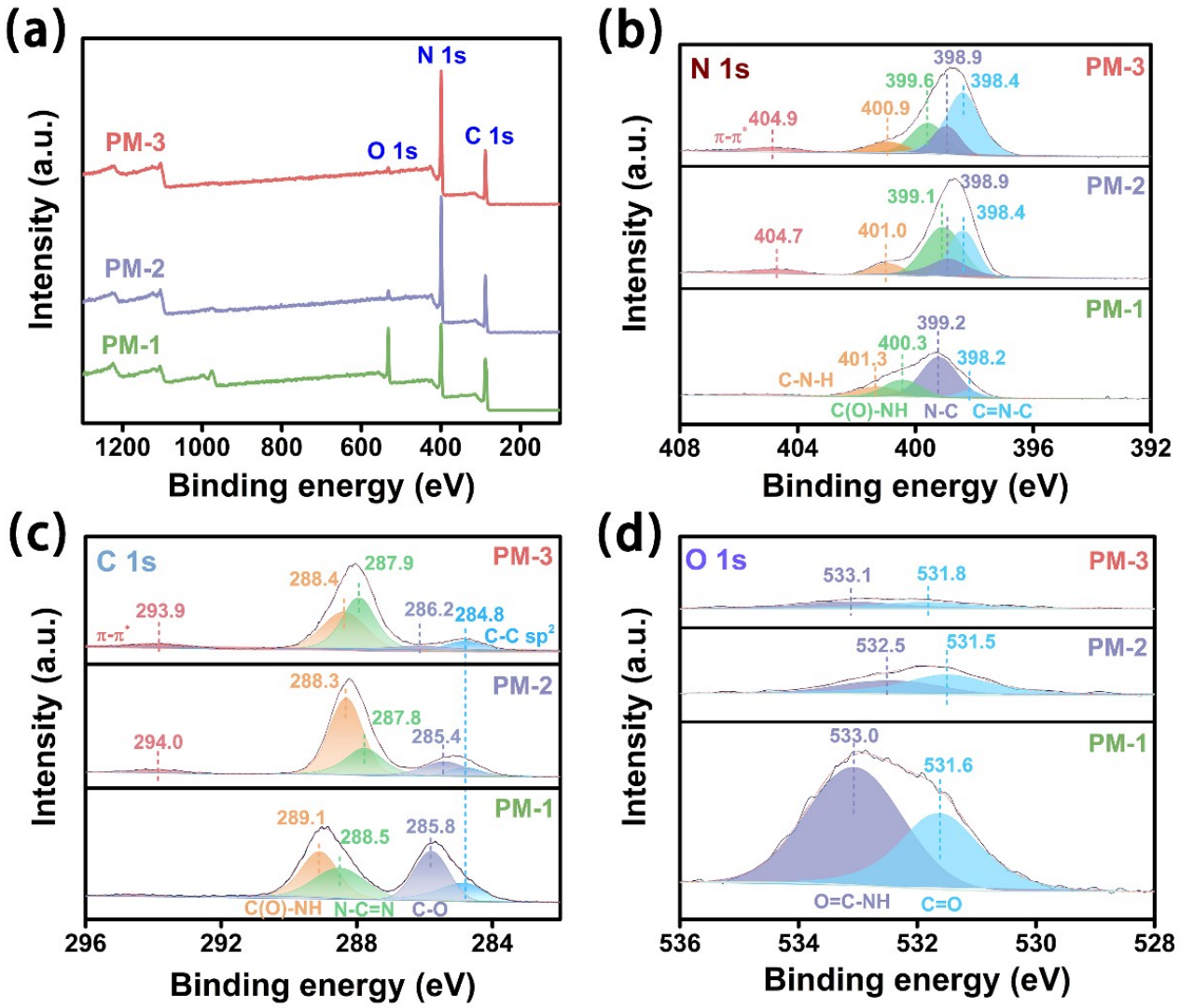

Figure S7. XPS spectra of (a) survey, (b) N 1s, (c) C 1s and (d) O 1s of PM-1, PM-2 and PM-3.

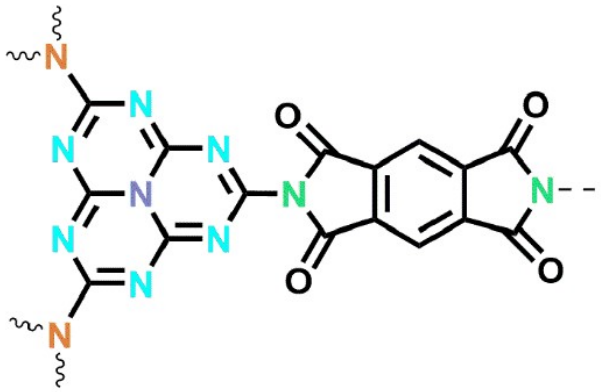

Figure S8. Schematic representation of different binding states of N element.

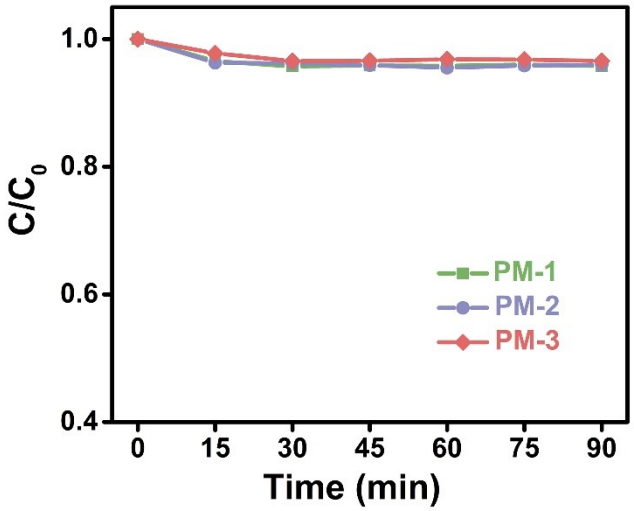

Figure S9. RhB adsorption curves of PM-1, PM-2 and PM-3.

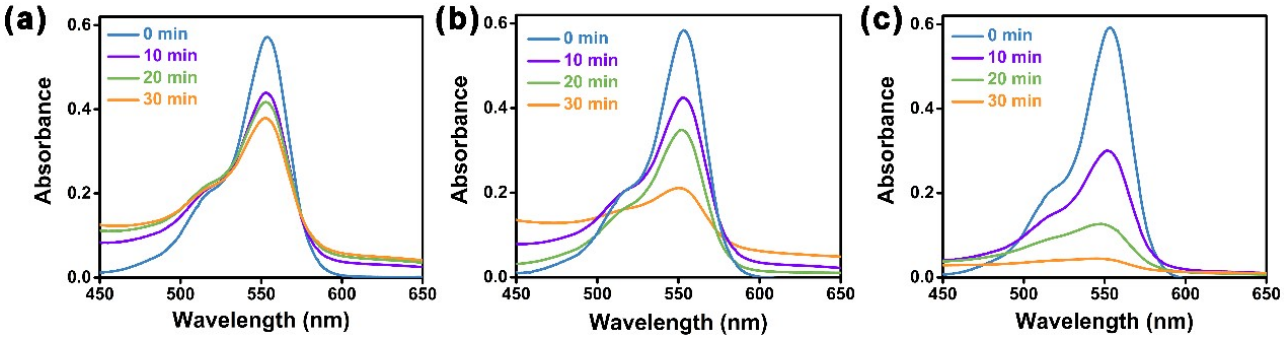

Figure S10. Time-dependent absorption spectra of piezocatalytic RhB degradation by (a) PM-1, (b) PM-2 and (c) PM-3.

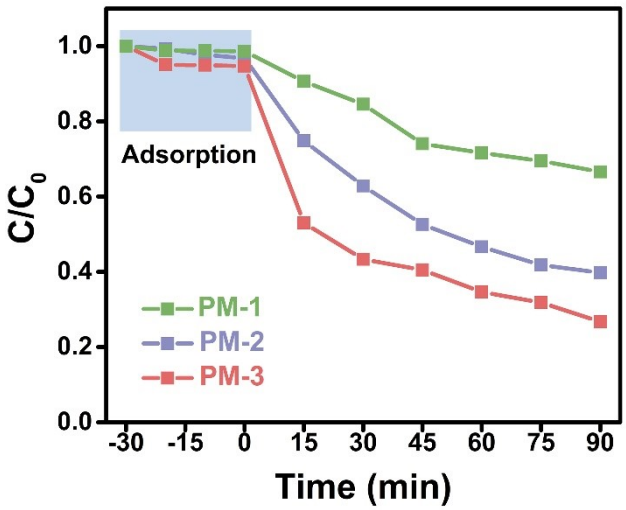

Figure S11. Piezo-degradation curves of PM-1, PM-2 and PM-3 for TC.

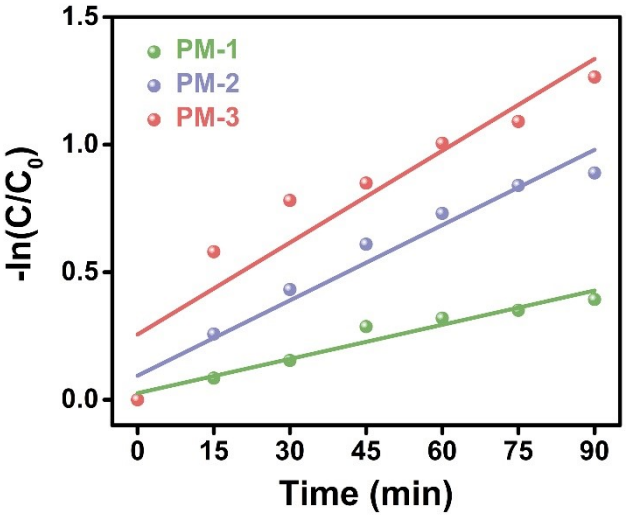

Figure S12. Reaction kinetic curves of PM-1, PM-2 and PM-3 for TC.

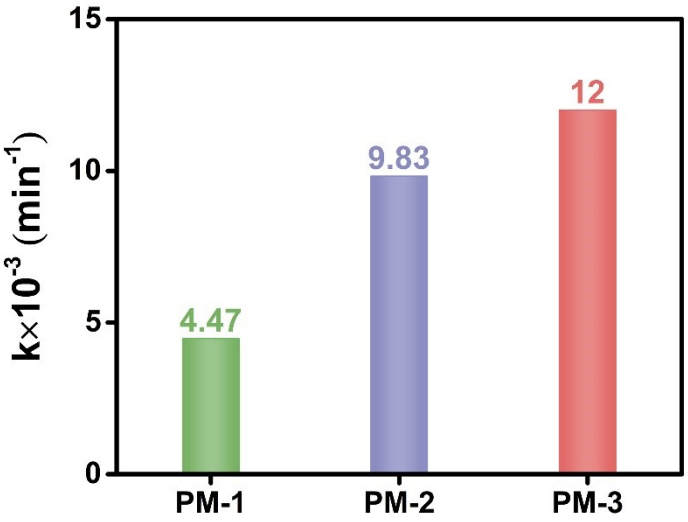

Figure S13. Apparent piezodegradation rate constants of PM-1, PM-2 and PM-3 for TC.

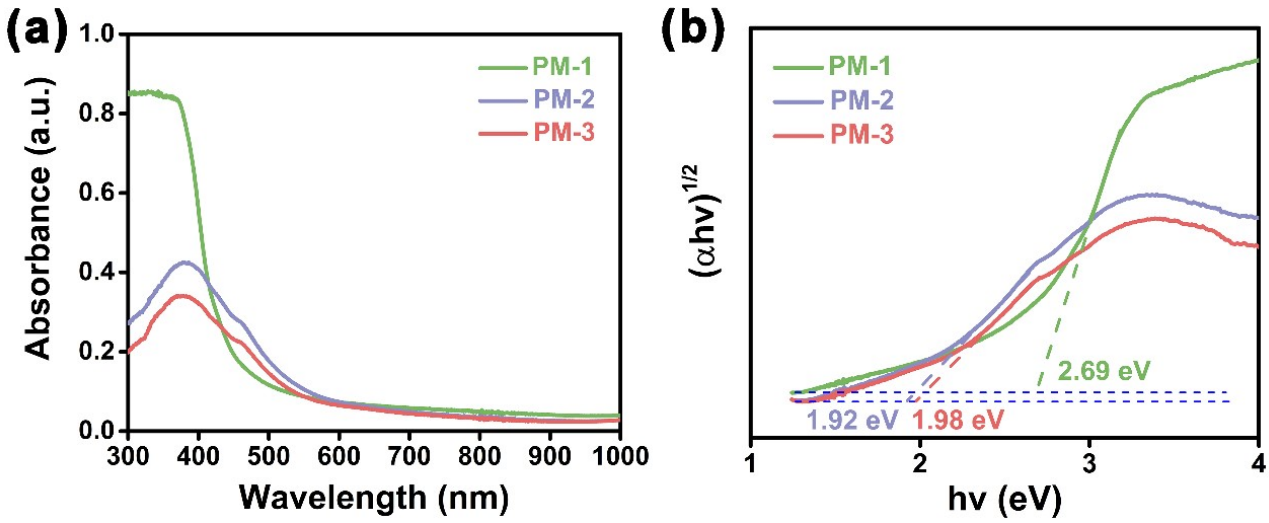

Figure S14. (a, b) UV-vis DRS spectra and corresponding bandgap of all PI samples.

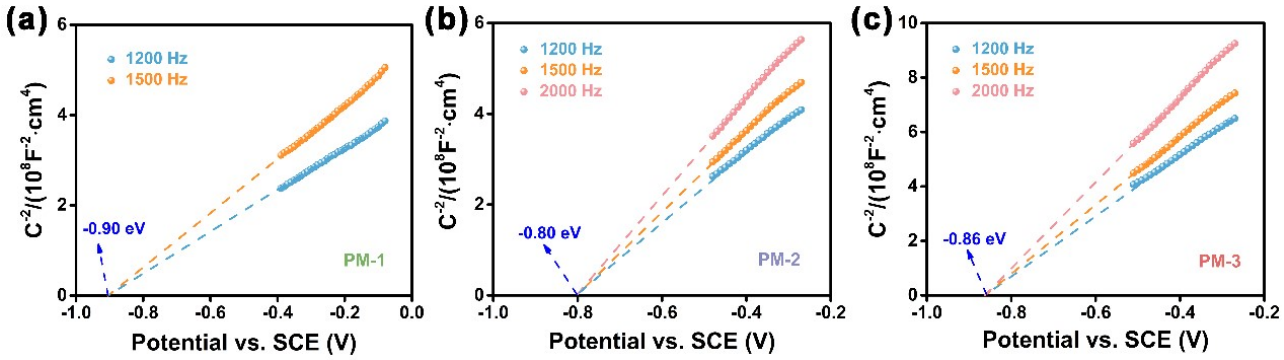

Figure S15. The Mott-Schottky plots of (a) PM-1, (b) PM-2 and (c) PM-3.

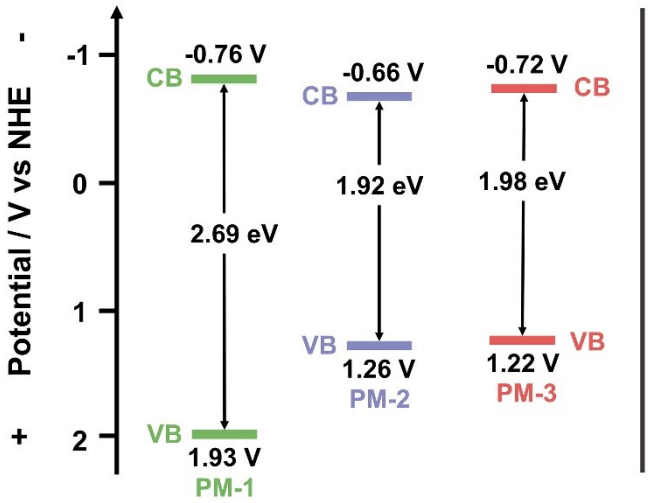

Figure S16. The band structure diagrams of all PI samples.

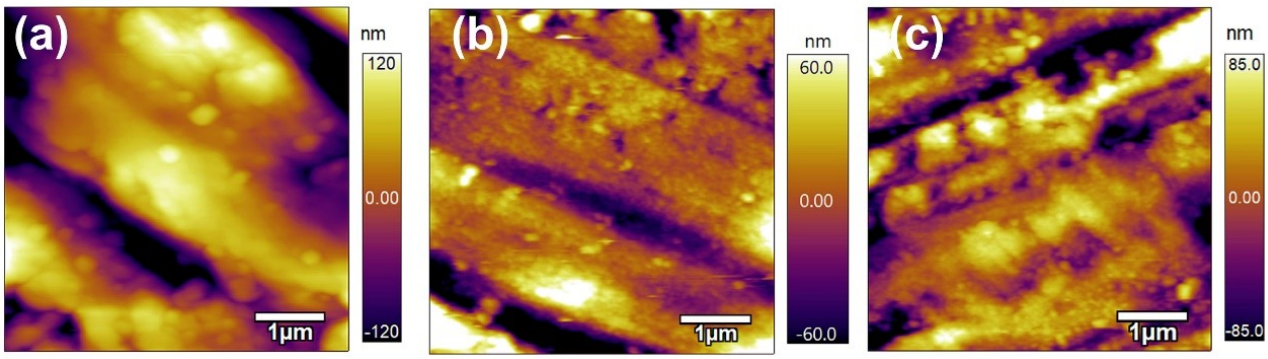

Figure S17. The PFM morphology images of (a) PM-1, (b) PM-2, (c) PM-3.

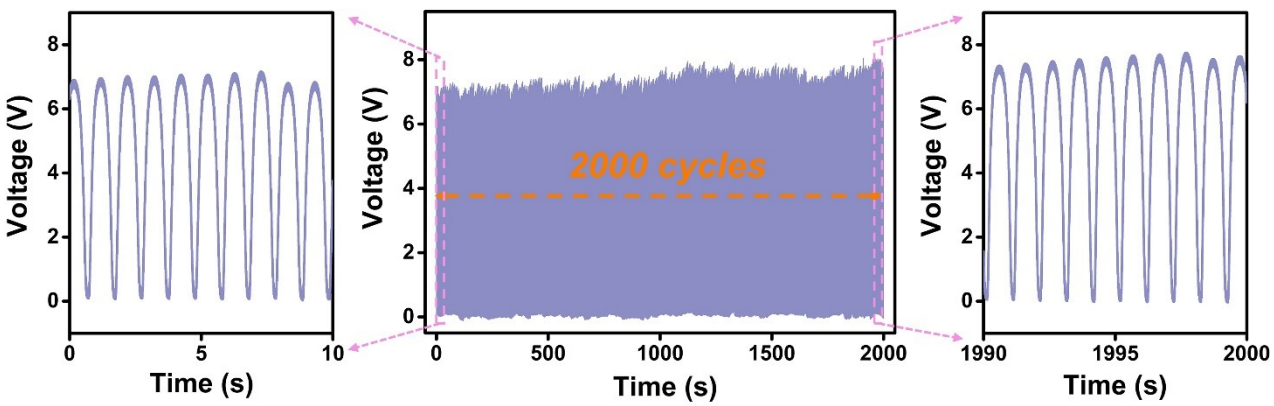

Figure S18. Endurance test of the PENG prepared by PM-3 for over 2000 cycles.

Table S1. Elemental contents of PI samples and g-C_3N_4.

Piezocatalyst	N (%)	C (%)	H (%)	O (%)
PM-1	31.57	42.77	2.37	23.30
PM-2	54.97	29.64	3.46	11.93
PM-3	57.96	29.93	3.30	8.82
g-C_3N_4 [2]	60.75	34.85	2.188	2.212

Table S2. Comparison of the RhB degradation performance of different piezocatalysts.

Piezocatalyst	Reaction system	Ultrasonic source	Reaction time (min)	k_{app} (min^{-1})	Ref.
PI	20 mg/L, 100 mL	40 kHz, 240 W	30	0.085	This work
g-C_3N_4	25 mg/L, 100 mL	40 kHz	120	0.021	[3]
PVDF	5 mg/L, 3.5 mL	70 W	120	≈0.027	[4]
PDA	5 mg/L, 50 mL	40 kHz, 120 W	20	0.012	[5]
PVDF-$ZnSnO_3$-Co_3O_4 mold	5 mg/L, 30 mL	33±3 kHz, 120 W	20	0.044	[6]
$BaTiO_3$-PDMS foam	5 mg/L, 40 mL	40 kHz, 400 W	120	0.022	[7]
$BaTiO_3$/C	5 mg/L, 50 mL	40 kHz, 150 W	40	0.049	[8]
$BaTiO_3$ nanofibers	5 mg/L, 20 mL	40 kHz, 240 W	60	0.054	[9]
$BaTiO_3$ dendrite	5 mg/L, 50 mL	40 kHz, 360 W	180	0.014	[10]
CoO_x/$BiFeO_3$	10 mg/L, 100 mL	40 kHz, 120 W	90	0.022	[11]
Ag/$PbBiO_2I$	10 mg/L, 100 mL	40 kHz, 120 W	90	0.017	[12]
BiOBr	10 mg/L, 50 mL	40 kHz, 120 W	120	0.006	[13]
$Na_{0.5}Bi_{0.5}TiO_3$	10 mg/L, 50 mL	40 kHz, 150 W	120	0.022	[14]
CdS/ZnO	10 mg/L, 100 mL	40 kHz, 120 W	90	0.067	[15]
$K_{0.5}Na_{0.5}NbO_3$	5 mg/L, 50 mL	40 kHz, 180 W	160	0.020	[16]
Bi_2WO_6 nanosheets	5 mg/L, 100 mL	40 kHz, 80 W	80	0.039	[17]

References

[1] S. Chu, C. Wang, J. Feng, Y. Wang and Z. Zou, *Int. J. Hydrog. Energy*., 2014, **39**, 13519-13526.

[2] W. Zhang, Z. Zhao, F. Dong and Y. Zhang, *Chin. J. Catal.*, 2017, **38**, 372-378.

[3] Y. Shao, C. Liu, H. Ma, J. Chen, C. Dong, D. Wang and Z. Mao, *Chem. Phys. Lett.*, 2022, **801**, 139748.

[4] B. Cromwell, M. Dubnicka, L. Sumathirathne, A. Thach and W. B. Euler, *J. Phys. Chem. C*., 2023, **27**, 11940-11947.

[5] Z. Kang, M. Chen, J. Wu, N. Qin and D. Bao, *J. Colloid Interface Sci.*, 2023, **650**, 169-181.

[6] T. D. Raju, S. Veeralingam and S. Badhulika, *ACS Appl. Nano Mater.*, 2020, **3**, 4777-4787.

[7] W. Qian, K. Zhao, D. Zhang, C. R. Bowen, Y. Wang and Y. Yang, *ACS Appl. Mater. Interfaces*., 2019, **11**, 27862-27869.

[8] L. Chen, Y. Jia, J. Zhao, J. Ma, Z. Wu, G. Yuan and X. Cui, *J. Colloid Interface Sci.*, 2021, **586**, 758-765.

[9] X. Wang, X. Gao, M. Li, S. Chen, J. Sheng and J. Yu, *Ceram. Int.*, 2021, **47**, 25416-25424.

[10] Z. Hu, W. Dong, Z. Dong, P. Li, Q. Bao and T. Cao, *Mater. Chem. Phys.*, 2023, **293**, 126911.

[11] L. Wang, J. Wang, C. Ye, K. Wang, C. Zhao, Y. Wu and Y. He, *Ultrason. Sonochem.*, 2021, **80**, 105813.

[12] Z. Li, Q. Zhang, L. Wang, J. Yang, Y. Wu and Y. He, *Ultrason. Sonochem.*, 2021, **78**, 105729.

[13] H. Lei, H. Zhang, Y. Zou, X. Dong, Y. Jia and F. Wang, *J. Alloy. Compd.*, 2019, **809**, 151840.

[14] L. Shi, C. Lu, L. Chen, Q. Zhang, Y. Li, T. Zhang and X. Hao, *J. Alloy. Compd.*, 2022, **895**, 162591.

[15] X. Li, J. Wang, J. Zhang, C. Zhao, Y. Wu and Y. He, *J. Colloid Interface Sci.*, 2022, **607**, 412-422.

[16] A. Zhang, Z. Liu, X. Geng, W. Song, J. Lu, B. Xie, S. Ke and L. Shu, *Ceram. Int.*, 2019, **45**, 22486-22492.

[17] Z. Kang, N. Qin, E. Lin, J. Wu, B. Yuan and D. Bao, *J. Clean Prod.*, 2020, **261**, 121125.